BIOCHEMISTRY
including biophysical chemistry & molecular biology

Article

pubs.acs.org/biochemistry

SB-RA-2001 Inhibits Bacterial Proliferation by Targeting FtsZ Assembly

Dipty Singh,[†] Anusri Bhattacharya,[†] Ankit Rai,[†] Hemendra Pal Singh Dhaked,[†] Divya Awasthi,[‡] Iwao Ojima,[‡] and Dulal Panda*[,†]

[†]Department of Biosciences and Bioengineering, Indian Institute of Technology Bombay, Mumbai 400076, India

[‡]Department of Chemistry and Institute of Chemical Biology & Drug Discovery, Stony Brook University, Stony Brook, New York 11794-3400, United States

Supporting Information

ABSTRACT: FtsZ has been recognized as a promising antimicrobial drug target because of its vital role in bacterial cell division. In this work, we found that a taxane SB-RA-2001 inhibited the proliferation of *Bacillus subtilis* 168 and *Mycobacterium smegmatis* cells with minimal inhibitory concentrations of 38 and 60 μM, respectively. Cell lengths of these microorganisms increased remarkably in the presence of SB-RA-2001, indicating that it inhibits bacterial cytokinesis. SB-RA-2001 perturbed the formation of the FtsZ ring in *B. subtilis* 168 cells and also affected the localization of the late cell division protein, DivIVA, at the midcell position. Flow cytometric analysis of the SB-RA-2001-treated cells indicated that the compound did not affect the duplication of DNA in *B. subtilis* 168 cells. Further, SB-RA-2001 treatment did not affect the localization of the chromosomal partitioning protein, Spo0J, along the two ends of the nucleoids and also had no discernible effect on the nucleoid segregation in *B. subtilis* 168 cells. The agent also did not appear to perturb the membrane potential of *B. subtilis* 168 cells. *In vitro*, SB-RA-2001 bound to FtsZ with modest affinity, promoted the assembly and bundling of FtsZ protofilaments, and reduced the GTPase activity of FtsZ. GTP did not inhibit the binding of SB-RA-2001 to FtsZ, suggesting that it does not bind to the GTP binding site on FtsZ. A computational analysis indicated that SB-RA-2001 binds to FtsZ in the cleft region between the C-terminal domain and helix H7, and the binding site of SB-RA-2001 on FtsZ resembled that of PC190723, a well-characterized inhibitor of FtsZ. The findings collectively suggested that SB-RA-2001 inhibits bacterial proliferation by targeting the assembly dynamics of FtsZ, and this can be exploited further to develop potent FtsZ-targeted antimicrobials.

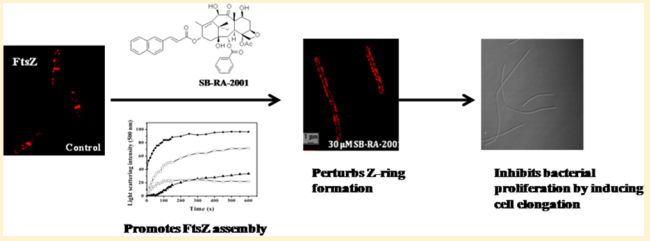

FtsZ is an essential protein of the bacterial cell division machinery. During cell division, it assembles into a contractile ring called the "Z-ring" at the midcell position.[1,2] Recent studies have recognized FtsZ as a promising antimicrobial drug target.[3−8] Several inhibitors of FtsZ that inhibit the proliferation of Gram-positive and Gram-negative bacteria by affecting FtsZ assembly dynamics have been identified.[7−18] Because FtsZ is strongly homologous to tubulin in structure but weakly similar to tubulin in sequence, small molecule inhibitors of FtsZ may also show activities against mammalian cells. However, inhibitors targeting FtsZ assembly in bacteria and not possessing much cytotoxicity toward mammalian cells as compared to bacterial cells should be qualified as suitable FtsZ-targeted agents.[19,20] In this regard, noncytotoxic taxanes can serve as potential molecules for the development of FtsZ inhibitors.[21] Different members of taxanes show different cytotoxic effects toward the proliferation of mammalian cells. For example, paclitaxel (Figure 1A), bearing an *N*-benzoylphenylisoserine moiety at C13, shows a very high level of cytotoxicity in mammalian cells, whereas taxane reversal agents (TRAs), bearing a hydrophobic 3-arylacrylic acid moiety at C13 or C7, are found to be noncytotoxic.[21] A library of 120 taxanes was designed, and their antibacterial properties against *Mycobacterium tuberculosis* (*Mtb*) cells were assessed.[6,22] The SB-RA series of TRAs having an (*E*)-3-(naphtha-2-yl)acryloyl (2-NpCH═CHCO) group at C13 demonstrated a MIC_{99} between 2.5 and 5 μM against drug-sensitive and drug-resistant *Mtb* strains.[6,22] On the basis of the MIC_{99} values and cytotoxicity assay, SB-RA-2001 (Figure 1A) was selected as a potential compound for antitubercular drug discovery. Further, the cytotoxic effect of SB-RA-2001 in human cancer cell lines was found to be significantly reduced (by 3 orders of magnitude) compared to that of paclitaxel.[22] Therefore, SB-RA-2001 could be used as a promising compound for the development of noncytotoxic taxane-based FtsZ-targeted antibacterial agents.[22]

This study evaluates the effects of SB-RA-2001 on FtsZ assembly and elucidates its antibacterial mechanism. SB-RA-2001 treatment induced cell elongation and inhibited bacterial cell proliferation without having any detectable effects on either

Received: October 2, 2013
Revised: March 16, 2014
Published: April 21, 2014

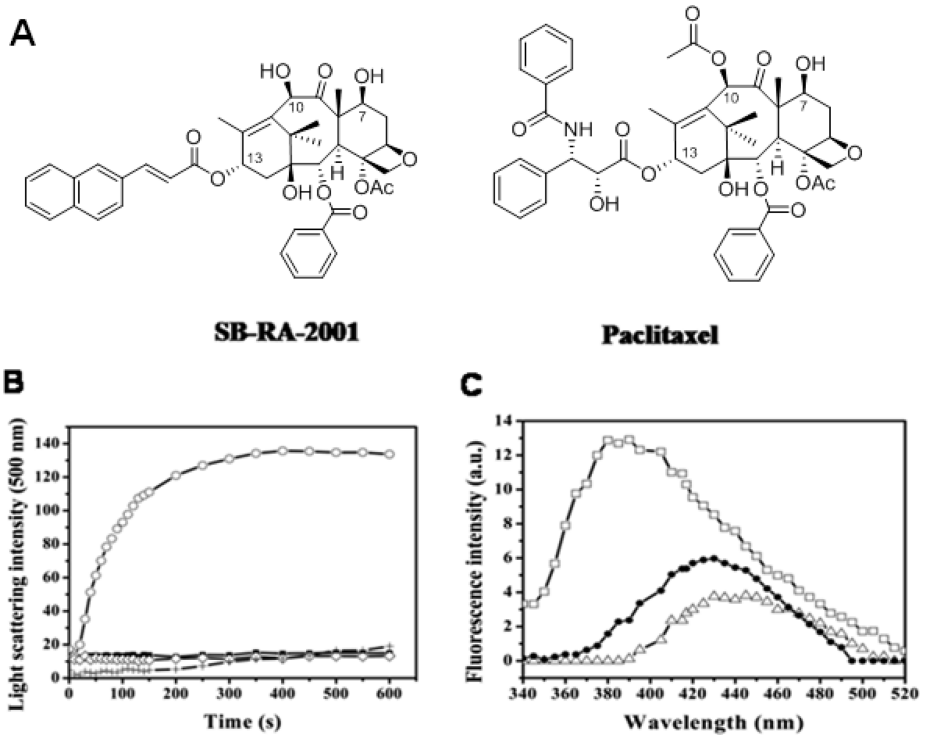

Figure 1. SB-RA-2001 exhibited characteristics on tubulin assembly and tubulin binding different from those of paclitaxel. (A) Structures of SB-RA-2001 [(*E*)-3-(naphtha-2-yl)acryloyl (2-NpCH═CHCO) group at C13] and paclitaxel. (B) Assembly of tubulin (10 μM) in the absence (■) and presence of 10 (◇) and 20 μM (+) SB-RA-2001 or 3 μM (○) paclitaxel monitored by light scattering. (C) Fluorescence spectra of 2 μM SB-RA-2001 in the absence (△) and presence of 5 μM tubulin (●) and 5 μM FtsZ (□).

DNA replication or nucleoid segregation. The results indicate that SB-RA-2001 perturbed Z-ring formation in bacteria by promoting the assembly and stability of FtsZ protofilaments. The study suggests that taxane derivatives have the potential to be developed as FtsZ-targeted antibacterial agents.

■ EXPERIMENTAL PROCEDURES

Materials. PIPES, GTP, PMSF, DAPI, lysozyme, Cy3-conjugated goat anti-rabbit secondary antibody, and propidium iodide were procured from Sigma-Aldrich (St. Louis, MO). IPTG was obtained from Calbiochem. Bio-Gel P4 and P6 resin was procured from Bio-Rad. Nickel-NTA was obtained from Qiagen. The rabbit polyclonal FtsZ antibody was obtained from Bangalore Genei. SB-RA-2001 was prepared by the previously reported method at the Ojima laboratory.[21] The Bac*Light* bacterial membrane potential kit was procured from Invitrogen. The Factor Xa cleavage capture kit was obtained from Novagen, EMD chemicals (San Diego, CA).

Preparation of the SB-RA-2001 Stock Solution. SB-RA-2001 was soluble in DMSO. A stock solution of 50 mM was prepared in 100% DMSO and subsequently diluted in aqueous buffer. No precipitate of SB-RA-2001 was visible up to 200 μM in PIPES buffer (pH 6.8).

Purification of *Bacillus subtilis* FtsZ. *B. subtilis* FtsZ was purified from *Escherichia coli* BL21(DE3) pLysS cells transformed with the pET16b vector.[18] Briefly, cells were grown in LB medium containing 12.5 μg/mL chloramphenicol and 100 μg/mL ampicillin and induced at the late log phase (OD_{600} = 0.8; 1 mM IPTG) for 6 h. The induced cells were harvested and lysed in ice-cold lysis buffer [50 mM NaH_2PO_4 (pH 8.0) and 300 mM NaCl] containing 0.1% β-ME, 2 mM PMSF, and 1 mg/mL lysozyme. The protein was purified using nickel-NTA agarose using elution buffer containing 25 mM PIPES (pH 6.8), 300 mM NaCl, and 250 mM imidazole. Purified protein was then desalted using the Biogel P6 resin pre-equilibrated with 25 mM PIPES and 50 mM KCl (pH 6.8). The concentration of purified FtsZ was determined by the Bradford method[23] using BSA as a standard. The concentration of the protein was finally adjusted using a correction factor of 1.2 for the FtsZ/BSA ratio.[24] FtsZ aliquots were stored at −80 °C. Prior to each experiment, FtsZ was centrifuged to remove aggregates.

Light Scattering Assay. Goat brain tubulin (10 μM) in 25 mM PIPES buffer (pH 6.8) and 5 mM $MgCl_2$ was incubated without and with paclitaxel (3 μM) and SB-RA-2001 (10 and 20 μM) at 4 °C for 10 min. The polymerization was initiated by adding 1 mM GTP to the reaction mixture, and the assembly of tubulin was monitored at 400 nm using a fluorescence spectrometer (FP-6500, JASCO, Tokyo, Japan) connected to a temperature-controlled bath at 37 °C.

The effect of SB-RA-2001 on the assembly kinetics of FtsZ *in vitro* was determined by 90° light scattering at 500 nm.[25,26] Briefly, FtsZ (3 μM) was incubated without or with different concentrations (20, 40, and 60 μM) of SB-RA-2001 in 25 mM PIPES (pH 6.8) containing 50 mM KCl and 5 mM $MgCl_2$ at 4 °C for 10 min. Then, 1 mM GTP was added to the reaction mixtures, and the kinetics of the assembly of FtsZ was monitored at 37 °C for 600 s. The light scattering traces of different concentrations of SB-RA-2001 in the absence of FtsZ were also recorded (Figure S1 of the Supporting Information). At higher concentrations, SB-RA-2001 showed some light scattering; however, the light scattering intensity was much higher in the presence of FtsZ than in its absence. The light scattering traces of SB-RA-2001 alone were subtracted from

dx.doi.org/10.1021/bi401356y | *Biochemistry* 2014, 53, 2979−2992

their respective data set with the protein. After assembly for 10 min, the reaction kinetics reached an apparent equilibrium, and the scattering intensity after assembly for 10 min was used to calculate the extent of assembly. Additionally, the initial rate of the increase in the light scattering intensity of the assembly of FtsZ in the absence and presence of SB-RA-2001 was determined from a linear plot of the light scattering intensity of FtsZ assembly for the first 100 s.

Dilution-Induced Disassembly Assay. FtsZ (5 μM) in 25 mM PIPES buffer (pH 6.8) containing 50 mM KCl, 5 mM $MgCl_2$, and 1 mM GTP was polymerized at 37 °C for 5 min. The preformed polymers were diluted five times in warm buffer [25 mM PIPES buffer (pH 6.8) containing 50 mM KCl, 5 mM $MgCl_2$, and 1 mM GTP] in the absence and presence of different concentrations (20, 40, and 60 μM) of SB-RA-2001 and incubated at 37 °C for 10 min. The polymers were collected through centrifugation (88760*g*) for 30 min at 30 °C, and the pellets were dissolved in sodium dodecyl sulfate polyacrylamide gel electrophoresis (SDS−PAGE) loading dye [0.25% bromophenol blue, 0.5 M DTT, 50% glycerol, and 10% SDS in 0.25 M Tris-HCl (pH 6.8)]. Samples were resolved via 12% SDS−PAGE, and the intensity of the bands was analyzed with ImageJ Pro Plus.

Sedimentation Assay. FtsZ (3 μM) was incubated without or with different concentrations (20, 40, and 60 μM) of SB-RA-2001 in 25 mM PIPES buffer (pH 6.8) containing 50 mM KCl and 5 mM $MgCl_2$ at 4 °C for 10 min. Polymerization was conducted in the presence of 1 mM GTP at 37 °C for 10 min. The polymers were collected by high-speed centrifugation (88760*g*) for 30 min at 30 °C. The pellets were dissolved in SDS−PAGE loading dye [0.25% bromophenol blue, 0.5 M DTT, 50% glycerol, and 10% SDS in 0.25 M Tris-HCl (pH 6.8)]. Samples were resolved via 12% SDS−PAGE, and band intensity was analyzed with ImageJ Pro Plus.

Characterization of Binding of SB-RA-2001 to FtsZ and Tubulin. Direct binding of SB-RA-2001 to FtsZ and tubulin was assessed using the increase in the fluorescence intensity of SB-RA-2001 upon binding to the proteins. SB-RA-2001 (2 μM) in 25 mM PIPES (pH 6.8) was incubated with either 5 μM FtsZ or 5 μM tubulin at 25 °C for 10 min. The fluorescence spectra were recorded in the range of 340−520 nm using 320 nm as an excitation wavelength using a fluorescence spectrometer (FP-6500, JASCO). The fluorescence spectra of the corresponding blanks were recorded and subtracted from the respective data sets. FtsZ and tubulin did not show significant fluorescence in the wavelength range of 340−520 nm. Further, to determine the effect of different concentrations of FtsZ on the fluorescence intensity of SB-RA-2001, SB-RA-2001 (1 μM) was incubated without and with (1, 2, 3, 4, and 5 μM) FtsZ in 25 mM PIPES (pH 6.8) at room temperature for 15 min. The reaction mixtures were excited at 320 nm, and the emission spectra were recorded in the range of 340−520 nm in a fluorescence spectrometer (FP-6500, JASCO).

The change in SB-RA-2001 fluorescence upon binding to FtsZ was used to determine the dissociation constant (K_d) of the SB-RA-2001−FtsZ interaction. FtsZ (2 μM) in 25 mM PIPES (pH 6.8) was incubated in the absence and presence of different concentrations of SB-RA-2001 (2−60 μM) for 15 min at 25 °C. After incubation for 15 min, fluorescence spectra were recorded in the range of 340−520 nm using 320 nm as an excitation wavelength. All fluorescence spectra were recorded using a cuvette with a path length of 0.3 cm. The spectra of equimolar amounts of SB-RA-2001 were recorded in the absence of FtsZ. The change in the fluorescence of SB-RA-2001 (ΔF) was calculated by subtracting the fluorescence of free SB-RA-2001 from that of SB-RA-2001 in the presence of FtsZ. The change in fluorescence (ΔF) at 400 nm was fit to the equation $\Delta F = (\Delta F_{max} L)/(K_d + L)$, where ΔF is the change in the fluorescence intensity of SB-RA-2001 when it is in equilibrium with FtsZ, ΔF_{max} is the maximal change in the fluorescence of SB-RA-2001 when the receptor site is fully occupied, and L is the concentration of SB-RA-2001. The dissociation constant of the interaction of FtsZ and SB-RA-2001 was determined using GraphPad Prism 5 (Graph Pad Software, San Diego, CA). Because SB-RA-2001 has an absorbance at 320 nm, the spectra were further corrected for the inner filter effect using the equation

$$F_{corrected} = F_{observed} \times \text{antilog}(\lambda_{ex} + \lambda_{em}/2)$$

where $F_{corrected}$ is the corrected fluorescence spectra of SB-RA-2001 after inner filter correction, $F_{observed}$ is the observed fluorescence of SB-RA-2001, and λ_{ex} and λ_{em} are the absorbance of SB-RA-2001 at its excitation and emission wavelengths, respectively.

Effect of GTP on the Binding of SB-RA-2001 to FtsZ. FtsZ (2 μM) was incubated in 25 mM PIPES (pH 6.8) containing 1 mM $MgCl_2$ and 200 mM NaCl without or with different concentrations of GTP (25−200 μM) on ice for 10 min. SB-RA-2001 (20 μM) was then added to each of the reaction mixtures, and they were again incubated at room temperature for 10 min. The change in the SB-RA-2001 fluorescence spectra was recorded in the range of 340−520 nm, keeping the excitation wavelength at 320 nm. Emission spectra of the corresponding blanks for each of the reaction sets were also recorded. The experiment was performed three times.

Electron Microscopy Analysis. FtsZ (3 μM) was incubated in PIPES buffer [25 mM PIPES (pH 6.8), 50 mM KCl, and 5 mM $MgCl_2$] without and with different concentrations (20 and 60 μM) of SB-RA-2001 at 4 °C for 10 min. Then, 1 mM GTP was added to each of the reaction mixtures, and polymerization was conducted at 37 °C for 10 min. The protein polymers were applied to Formvar carbon-coated copper grids (300 mesh) for 30 s and blotted dry. The sample-containing grids were then negatively stained with 1% uranyl acetate for 30 s, dried, and observed under a JEM 2100 ultra HRTEM instrument at 200 kV.

FITC Labeling of FtsZ. FtsZ contains several lysine residues,[27] and one or more of these lysine residues can be covalently modified with FITC.[28] Briefly, FtsZ (20 μM) was incubated with FITC (80 μM) in 25 mM PIPES (pH 6.8) for 4 h on ice. Then, the reaction was quenched with 5 mM Tris-HCl. The unbound FITC was removed in two steps: by being passed through a size exclusion column (P4 resin) and then by dialysis against 25 mM PIPES (pH 6.8). The concentration of FITC-bound FtsZ was estimated by monitoring the absorbance of FITC at 495 nm (molar extinction coefficient of 77000 M^{-1} cm^{-1}). The incorporation ratio of FITC per FtsZ molecule was calculated by dividing the concentration of FtsZ-bound FITC by that of total FtsZ.[28]

Fluorescence Microscopy. FITC-FtsZ (3 μM) was incubated without and with varying concentrations (20, 40, and 60 μM) of SB-RA-2001 in 25 mM PIPES (pH 6.8), 50 mM KCl, and 5 mM $MgCl_2$ on ice for 10 min. Polymerization was initiated by adding 1 mM GTP to the reaction mixtures and incubating them at 37 °C for 10 min. The polymeric

dx.doi.org/10.1021/bi401356y | *Biochemistry* 2014, 53, 2979−2992

suspensions (10 μL) were then mounted on glass slides and observed using a fluorescence microscope (Eclipse TE2000-U microscope, Nikon, Tokyo, Japan).

GTPase Assay. The C-terminal histidine tag of FtsZ was removed using Factor Xa cleavage capture kit as described recently.[18] The GTP hydrolysis rate of histidine-tagged *Bs*FtsZ and untagged FtsZ was determined by the standard malachite green/ammonium molybdate assay.[26,29] Both histidine-tagged FtsZ and untagged FtsZ (6 μM) were polymerized at 37 °C in 25 mM PIPES buffer (pH 6.8) containing 50 mM KCl, 5 mM $MgCl_2$, and 1 mM GTP, and the moles of inorganic phosphate released at various time intervals (1, 3, 5, 10, and 15 min) were determined as described previously.[26] The GTPase activities of His-tagged FtsZ (1.5 ± 0.6 min^{-1}) and untagged FtsZ (1.7 ± 0.5 min^{-1}) were found to be similar, indicating that the histidine tag does not influence the GTPase activity of FtsZ.

The effects of SB-RA-2001 on the GTPase activity of FtsZ were determined by the malachite green/ammonium molybdate assay.[26,29] Briefly, FtsZ (3 μM) was incubated without and with different concentrations (20, 40, and 60 μM) of SB-RA-2001, and the moles of inorganic phosphate released after assembly for 5 min were determined as described above.

Some of the FtsZ-targeted agents have been reported to form colloidal aggregates under assembly conditions.[19] Triton X-100 is used to solubilize the aggregates of the compounds in enzymatic assays.[19] Therefore, the effect of SB-RA-2001 on the GTPase activity of FtsZ was also determined in the presence of 0.01% (v/v) Triton X-100.[19] Initially, SB-RA-2001 (20, 40, and 60 μM) in 25 mM PIPES (pH 6.8), 50 mM KCl, and 5 mM $MgCl_2$ was incubated with 0.01% Triton X-100 at 37 °C for 30 min. Following the incubation, the reaction sets were subjected to centrifugation at 14000*g* for 20 min, and the supernatants were collected. Subsequently, FtsZ (3 μM) was added to the supernatant having different concentrations of SB-RA-2001 and incubated for 15 min. The polymerization reaction was then initiated by the addition of 1 mM GTP to the reaction sets, and polymerization continued for 5 min at 37 °C. The moles of inorganic phosphate released were determined as described previously.[26]

Circular Dichroism (CD) Spectroscopy. FtsZ (5 μM) was incubated in the absence and presence of 10 and 20 μM SB-RA-2001 in 25 mM phosphate buffer (pH 6.5) for 10 min at 25 °C. The far-UV CD spectrum was recorded (200−250 nm) using a 0.1 cm path length quartz cuvette in a JASCO J-810 spectropolarimeter. The CD spectra were deconvoluted using CDNN, SSE software from JASCO. Each spectrum was an average of five scans, and the experiment was repeated three times.

Docking Methodology. The molecular docking tool AutoDock4.2[30] was used to identify the putative binding site of SB-RA-2001 on the *B. subtilis* FtsZ monomer. The three-dimensional coordinates of SB-RA-2001 were prepared using the PRODRG server.[31] The X-ray structures of *Bs*FtsZ [Protein Data Bank (PDB) entry 2RHL, A chain][32] and *Sa*FtsZ (PDB entry 4DXD)[33] were used as models for docking analysis. In *Sa*FtsZ, PC190723 was also present in addition to FtsZ and GDP. PC190723 was extracted prior to the docking simulation. The entire surface of FtsZ was covered in a grid box with dimensions of 170 Å × 170 Å × 170 Å with a grid spacing of 0.375 Å. SB-RA-2001 and PC190723 were used as flexible molecules, and FtsZ was considered as a rigid molecule for the docking analysis. The Lamarckian genetic algorithm was used for docking with default parameters. The docking of SB-RA-2001 and PC190723 to FtsZ was performed by conducting 50 independent jobs, each including 100 runs and yielding 5000 conformations. The clustering of these conformations was performed at a root-mean-square deviation (rmsd) of 6 Å. The clusters having more than 100 conformations were further selected on the basis of binding energy. Finally, the best cluster with minimal energy was chosen for further analysis. The interaction of SB-RA-2001 with FtsZ was analyzed using PyMol.[34] In addition, the structure of *Bs*FtsZ (PDB entry 2RHL), in which docked SB-RA-2001 is present (consisting of docked SB-RA-2001 and GDP), was superimposed on that of β-tubulin. The β-tubulin with GDP and paclitaxel was extracted from tubulin of *Bos taurus* (PDB entry 1JFF).[35]

Effect of SB-RA-2001 on Bacterial Cell Proliferation. *B. subtilis* 168 cells were grown overnight in LB broth at 37 °C and then inoculated into fresh LB tubes at an initial OD_{600} of 0.1. The cells were grown in the absence and presence of different concentrations of SB-RA-2001 for 4 h at 37 °C. The inhibition of cell proliferation was monitored by measuring OD_{600}, and the percent inhibition of cell proliferation was calculated using the formula

$$\%\text{inhibition} = 1 - [(N_t - N_0)/(N_c - N_0)] \times 100$$

where N_t and N_c are the absorbances of SB-RA-2001-treated and untreated *B. subtilis* 168 cells, respectively, after 4 h and N_0 is the OD_{600} at time zero. The concentration of SB-RA-2001, at which 50% inhibition of *B. subtilis* 168 cells was observed, was determined to be its half-maximal inhibitory concentration (IC_{50}).

Determination of the Minimal Inhibitory Concentration (MIC). The MIC values of SB-RA-2001 for *B. subtilis* 168 and *Mycobacterium smegmatis* cell proliferation were determined by the agar dilution method.[36] Briefly, *B. subtilis* 168 and *M. smegmatis* were grown in liquid medium (LB and Middlebrook 7H9 broth, respectively) for 16 h at 37 °C. The cell densities of the bacterial cultures were calculated from OD_{600} (1 OD_{600} unit = 1 × 10^9 cells/mL), and cultures were serially diluted to a final cell density of 1 × 10^6 cells/mL; 10^5 cells of *B. subtilis* 168 and *M. smegmatis* were then plated onto LB and Middlebrook 7H9 agar plates, respectively, containing various concentrations of SB-RA-2001. The plates were incubated at 37 °C for 12 h for *B. subtilis* 168 cells and 36 h for *M. smegmatis* cells. The concentration of SB-RA-2001 at which no colonies were observed was considered the MIC. The experiment was performed in triplicate.

Visualization of Morphological Changes in Bacteria. Morphological changes in *B. subtilis* 168 and *M. smegmatis* cells incubated with vehicle (0.1% DMSO) and 20 μM SB-RA-2001 were observed.[10] LB and Middlebrook 7H9 broth media were inoculated with microbial cultures of *B. subtilis* 168 and *M. smegmatis* cells, respectively, grown overnight and incubated (4 and 16 h) at 37 °C. The cells were fixed at 25 °C using 2.8% formaldehyde and 0.04% glutaraldehyde, and then, the cells were pelleted, washed, and resuspended in PBS (pH 7.4). The cell morphology was observed by a differential interference contrast microscope (Eclipse TE2000-U microscope, Nikon) at a 60× magnification. The cell length was measured using Image-Pro Plus (Media Cybernetics, Silver Spring, MD).

Effect of SB-RA-2001 on Z-Ring Formation and Nucleoid Segregation. Immunofluorescence microscopy was performed to visualize the effect of SB-RA-2001 on Z-ring formation and nucleoid segregation.[9] For visualization of the Z-ring, LB tubes were inoculated with *B. subtilis* 168 cells

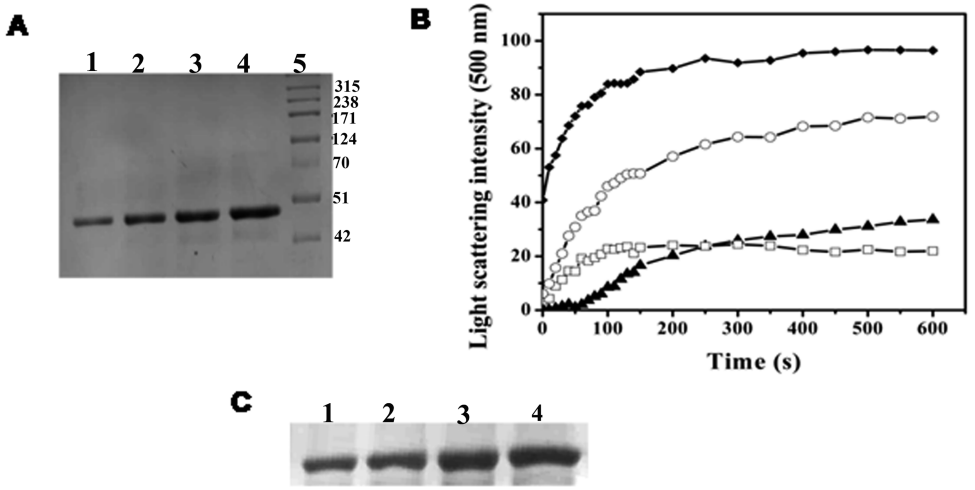

Figure 2. SB-RA-2001 promoted the assembly of FtsZ *in vitro*. (A) SB-RA-2001 reduced the level of dilution-induced disassembly of preformed FtsZ polymers. Lanes 1−4 show the amounts of FtsZ polymers recovered after dilution-induced disassembly in the absence of SB-RA-2001 and in the presence of 20, 40, and 60 μM SB-RA-2001, respectively. Lane 5 contained the protein molecular mass markers (kilodaltons). The experiment was performed three times. (B) Assembly of FtsZ in the absence (▲) and presence of 20 (□), 40 (○), and 60 μM (◆) SB-RA-2001 monitored by 90° light scattering. The experiment was performed three times. (C) FtsZ (3 μM) was polymerized without or with different concentrations of SB-RA-2001. Lanes 1−4 show the amounts of FtsZ polymerized in the absence of SB-RA-2001 and in the presence of 20, 40, and 60 μM SB-RA-2001, respectively. The experiment was conducted in triplicate.

(OD_{600} = 0.1) and further incubated for 4 h in the presence of vehicle (0.1% DMSO) and 20 and 30 μM SB-RA-2001. The cells were then fixed using 2.8% formaldehyde and 0.04% glutaraldehyde for 30 min at room temperature. Staining of cytoplasmic FtsZ was performed with a polyclonal FtsZ antibody (1:50) developed in rabbit, followed by staining with a Cy3-conjugated goat anti-rabbit secondary antibody (1:200). Nucleoids were stained using DAPI (20 μg/mL) and superimposed with Cy3 secondary antibody-stained FtsZ to obtain the merged image. The quantitation of Z-ring formation and nucleoid segregation was achieved by scoring 200 bacterial cells under each experimental condition.

GFP-tagged Spo0J in *B. subtilis* 168 strain HM160 cells (a gift from L. Hamoen, Newcastle University, Newcastle upon Tyne, U.K.) was grown (Casein Hydrolysate Broth containing 2 mg/L kanamycin) at 37 °C in the presence of 0.1% DMSO (vehicle) and 20 μM SB-RA-2001 for 4 h. *B. subtilis* Spo0J cells were harvested and fixed similarly as mentioned above. Nucleoid staining was achieved with 20 μg/mL DAPI. Images were captured using a confocal laser scanning microscope (Olympus, IX 81 with FV-500) at a 60× magnification. Merged images of individual cells were obtained by superimposing GFP-tagged Spo0J and DAPI-stained nucleoids.

FACS Analysis. Fresh LB tubes were inoculated with a culture of *B. subtilis* 168 cells grown overnight in the absence and presence of 20 μM SB-RA-2001 at 37 °C for 4 h. The cells were collected and fixed using a fixing solution (2.8% formaldehyde and 0.04% glutaraldehyde). Untreated and treated cells were permeabilized by subsequent treatments with PBS containing 0.1% Triton X-100 and PBS in the presence of lysozyme and EDTA, respectively. The permeabilized cells were then incubated with 50 μg/mL propidium iodide for 1 h at 25 °C in dark. Flow cytometry was performed using FACS Aria (Beckton Dickinson). Analysis of the data was performed using FCS express 4 (research edition, trial version). The median fluorescence intensity of propidium iodide (PI) was used to analyze the change in the DNA content of the SB-RA-2001-treated cells with respect to the DNA content of the control cells. The experiment was repeated twice.

Effect of SB-RA-2001 on Late Cell Division Protein DivIVA. GFP-tagged DivIVA in *B. subtilis* 168 strain 1803 cells (a gift from L. Hamoen) was grown (Casein Hydrolysate Broth) to an OD_{600} of 0.1 at 37 °C in the presence of 12.5 mg/L chloramphenicol. Subsequently, the cells were grown in the presence of a vehicle (0.1% DMSO) or 20 μM SB-RA-2001 for 1 h. The cells were then harvested, fixed, and stained for FtsZ. Images were captured using a confocal laser scanning microscope (Olympus, IX 81 with FV-500) at a 60× magnification. The images of GFP-tagged DivIVA and Cy3 secondary antibody-stained FtsZ of individual cells were superimposed on each other to obtain the merged image.

Effect of SB-RA-2001 on the Membrane Potential of *B. subtilis* 168 Cells. Inhibition of bacterial cell proliferation can be caused by a perturbed membrane potential in cells.[37] The effect of SB-RA-2001 on the membrane potential of *B. subtilis* 168 cells was determined using a fluorescent probe, 3,3′-diethyloxacarbocyanine iodide ($DiOC_2$). $DiOC_2$ exhibits green fluorescence in the monomeric state, and an increase in membrane potential is known to induce self-association of the dye that accompanies the red shift in the spectrum.[38,39] Therefore, the membrane potential of *B. subtilis* 168 cells in the absence and presence of SB-RA-2001 was determined using the change in $DiOC_2$ fluorescence.[38] Briefly, a culture of *B. subtilis* 168 cells grown overnight was inoculated into fresh LB tubes and grown at 37 °C for 2 h. Cells (1×10^5) were resuspended in filtered PBS and further incubated without or with a positive control (0.2 μM), carbonyl cyanide 3-chlorophenylhydrazone (CCCP), or SB-RA-2001 (20 and 30 μM) at 25 °C for 30 min. Then, 12 μM $DiOC_2$ was added to each of the reaction sets, and the mixtures were further incubated for 30 min in the dark. The reaction mixtures were excited at 470 nm, and the fluorescence emission spectra (500−550 nm) were monitored. Spectra of the respective blanks were also recorded.

Mammalian Cell Proliferation Assay. Human cervical carcinoma (HeLa) cells were cultured in MEM medium

dx.doi.org/10.1021/bi401356y | *Biochemistry* 2014, 53, 2979−2992

supplemented with 10% FBS and a 1% antibacterial and antifungal solution.[40] Cells were kept in a humidified 5% CO_2 incubator at 37 °C. To evaluate the effect of SB-RA-2001 on the proliferation of HeLa cells, 1×10^5 cells per milliliter were grown without or with different concentrations of SB-RA-2001 for 24 h in a 96-well cell culture plate. After incubation, cells were fixed, and the effect of different concentrations of SB-RA-2001 on mammalian cell proliferation was measured by the sulforhodamine B assay.[40,41] Data were averages of three independent experiments. Under similar experimental conditions, effects of paclitaxel on HeLa cell proliferation were also evaluated.

RESULTS

SB-RA-2001 Did Not Promote the Assembly of Tubulin and Bound Very Weakly to Tubulin *in Vitro*. Paclitaxel (Figure 1A) is known to promote the assembly of tubulin and to stabilize microtubules.[42] SB-RA-2001 (Figure 1A) had no detectable effect on the assembly of purified tubulin (Figure 1B). SB-RA-2001 was found to exhibit an intrinsic fluorescence at 400 nm. The increase in SB-RA-2001 fluorescence at 400 nm upon binding to tubulin or FtsZ was used as a tool to assess the interaction of SB-RA-2001 with tubulin and FtsZ (Figure 1C). The preliminary experiment indicated that SB-RA-2001 binds to FtsZ more efficiently than to tubulin (Figure 1C). The cytotoxicity of SB-RA-2001 against proliferation of mammalian cells was determined by growing HeLa cells in the absence and presence of SB-RA-2001. The half-maximal inhibitory concentration (IC_{50}) of the proliferation of HeLa cells occurred in the presence of 45 ± 5 μM compound. The concentration of SB-RA-2001 required to inhibit the proliferation of HeLa cells by 100% was determined to be 135 ± 10 μM. The effect of paclitaxel on HeLa cell proliferation was also examined, and the IC_{50} was determined to be 12 ± 2 nM. The results together indicated that SB-RA-2001 interacted with tubulin and microtubules very weakly.

SB-RA-2001 Prevented the Disassembly of Preformed FtsZ Polymers. FtsZ polymers are known to disassemble upon dilution. SB-RA-2001 suppressed dilution-induced disassembly of preformed FtsZ polymers (Figure 2A). For example, the recovery of FtsZ polymers was found to increase by 13 ± 5, 22 ± 7, and 46 ± 4% compared to the control in the presence of 20, 40, and 60 μM SBRA-2001, respectively, indicating that SB-RA-2001 can stabilize FtsZ polymers.

SB-RA-2001 Promoted the Assembly and Bundling of FtsZ Protofilaments *in Vitro*. Because SB-RA-2001 stabilizes FtsZ polymers, we checked whether it could promote FtsZ assembly (Figure 2B). The light scattering traces of FtsZ assembly kinetics in the absence and presence of different concentrations of SB-RA-2001 indicated that SB-RA-2001 enhanced the assembly of FtsZ (Figure 2B and Figure S1 of the Supporting Information). For example, the light scattering intensity of FtsZ (3 μM) was increased by 51 ± 23% in the presence of 40 μM SB-RA-2001 compared to the control. Further, SB-RA-2001 appeared to increase the initial rate of FtsZ assembly. For example, the initial rate of increase in the light scattering intensity of FtsZ assembly for the first 100 s was determined to be 0.07, 0.19, and 0.38 au/s in the absence of SB-RA-2001 and in the presence of 20 and 40 μM SB-RA-2001, respectively. The sedimentable polymer mass of FtsZ also increased in the presence of SB-RA-2001 compared to the control, indicating that SB-RA-2001 enhances the assembly of FtsZ *in vitro* (Figure 2C). The amount of polymerized FtsZ was found to increase by 20 ± 10, 23 ± 15, and 30 ± 10% in the presence of 20, 40, and 60 μM SB-RA-2001, respectively. Additionally, electron microscopy analysis of FtsZ assembly revealed that the assembly of FtsZ was enhanced in the presence of SB-RA-2001 (Figure S2A of the Supporting Information). The extent of bundling as well as the number of polymers of FtsZ per field of view was found to increase significantly in the presence of 20 and 60 μM SB-RA-2001 compared to those of the control. This observation was also supported well by fluorescence microscopy studies in which SB-RA-2001 was found to increase the level of assembly of FITC-FtsZ in a concentration-dependent manner (Figure S2B of the Supporting Information).

SB-RA-2001 Suppressed the GTPase Activity of FtsZ *in Vitro*. Because the assembly dynamics of FtsZ is regulated by its GTPase activity,[1] the effect of SB-RA-2001 on the GTP hydrolysis rate of FtsZ assembly was examined (Figure 3). SB-RA-2001 was found to suppress the GTPase activity of FtsZ in a concentration-dependent fashion. Further, to confirm that the inhibition of the GTPase activity of FtsZ observed in the presence of SB-RA-2001 was not due to the self-aggregation of the compound, the GTPase assay was also performed in the presence of 0.01% Triton X-100.[19] The inhibition of the GTPase activity of FtsZ by SB-RA-2001 was found to be similar in the absence and presence of 0.01% Triton X-100 (Figure 3). For example, 20, 40, and 60 μM SB-RA-2001 inhibited the GTPase activity of FtsZ by 25 ± 7.8, 51 ± 9.4, and 65 ± 13%, respectively, in the absence of 0.01% Triton X-100, while these concentrations of SB-RA-2001 inhibited the GTPase activity of FtsZ by 36 ± 1.4, 53 ± 7, and 64.6 ± 4%, respectively, in the presence of 0.01% Triton X-100.

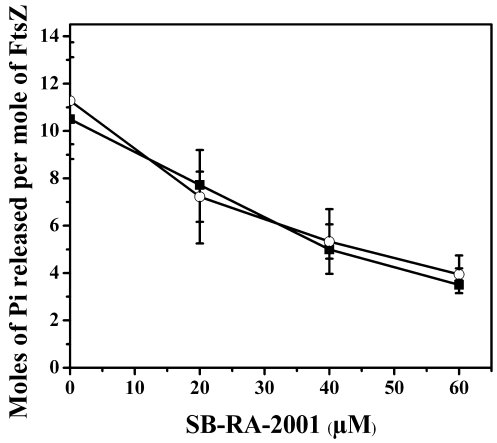

Figure 3. SB-RA-2001 suppressed the GTPase activity of FtsZ. The effects of SB-RA-2001 on the GTPase activity of FtsZ without (■) and with 0.01% (v/v) Triton X-100 (○) were determined after assembly for 5 min. The data are from three sets of experiments.

SB-RA-2001 Bound to FtsZ *in Vitro*. A fixed concentration of SB-RA-2001, upon incubation with different concentrations of FtsZ, showed a concentration-dependent increase in the fluorescence intensity of SB-RA-2001 (Figure 4A). The fluorescence emission maximum of SB-RA-2001 was found to be 440 and 400 nm in the absence and presence of 5 μM FtsZ, respectively. SB-RA-2001 showed a large blue shift in its emission maximum upon interacting with FtsZ, and the fluorescence intensity was also enhanced, suggesting that SB-RA-2001 binds to FtsZ.

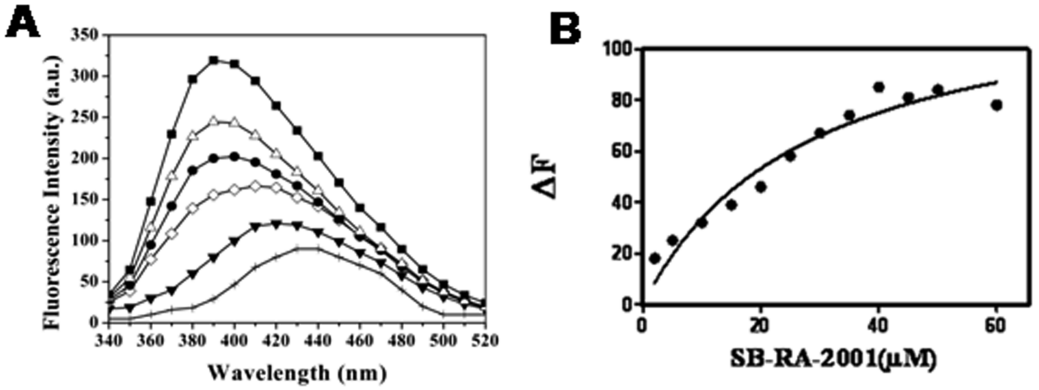

Figure 4. Binding interaction of SB-RA-2001 and FtsZ monitored by fluorescence spectroscopy. (A) FtsZ increased the fluorescence intensity of SB-RA-2001. The fluorescence spectra of 1 μM SB-RA-2001 in the absence of FtsZ (+) and in the presence of 1 (◀), 2 (◇), 3 (●), 4 (△), and 5 (■) μM FtsZ are shown. (B). FtsZ (2 μM) was incubated with different concentrations of SB-RA-2001 for 15 min at 25 °C. The change in the fluorescence intensity of the FtsZ−SB-RA-2001 complex is plotted vs SB-RA-2001 concentration.

A fixed concentration of FtsZ was incubated with varying concentrations of SB-RA-2001 to determine the dissociation constant of the interaction of SB-RA-2001 with FtsZ. The dissociation constant of the interaction of SB-RA-2001 with FtsZ was determined by monitoring the increase in SB-RA-2001 fluorescence upon binding to FtsZ. The data were then fit to a binding isotherm, and a dissociation constant of 29 ± 2 μM was estimated for the interaction of SB-RA-2001 with FtsZ, suggesting that the ligand binds to FtsZ with a modest affinity (Figure 4B).

The effect of GTP on the binding of SB-RA-2001 to FtsZ was determined by monitoring the fluorescence intensity of SB-RA-2001 upon binding to FtsZ at 400 nm (Figure S3 of the Supporting Information). The increase in the fluorescence intensity of SB-RA-2001 in the presence of FtsZ was found to be similar without or with different concentrations of GTP, indicating that SB-RA-2001 does not compete with GTP for its binding to FtsZ (Figure S3 of the Supporting Information). We have also measured the fluorescence of SB-RA-2001 in the presence of FtsZ at 460 nm. The fluorescence of the FtsZ−SB-RA-2001 complex (at 460 nm) did not change in the absence or presence of GTP, indicating that GTP did not compete for binding at the same site on FtsZ. Further, SB-RA-2001 did not have any effect on the secondary structure of FtsZ as the far-UV CD spectrum of FtsZ was found to be unaltered in the presence of varying concentrations of SB-RA-2001 (data not shown).

Putative Binding Site of SB-RA-2001 on FtsZ. Initially, docking of PC190723 was performed on *Sa*FtsZ as a control (Figure S4 of the Supporting Information). The PC190723 topology was extracted from *Sa*FtsZ (PDB entry 4DXD).[33] The docked conformation of PC190723 was compared with the X-ray crystallographically determined structure (Figure S4 of the Supporting Information and Table 1), and the root-mean-square deviation (rmsd) between docked PC190723 and crystallized PC190723 was estimated to be 0.951 Å, indicating appropriate docking.[30,43] Further, docking of SB-RA-2001 and PC190723 on *Bs*FtsZ (PDB entry 2RHL)[32] was performed using a similar methodology.

Table 1. Residues of *Sa*FtsZ Lying within 4 Å of PC190723[a]

crystal PC190723	**Gln192**, **Gly193**, **Gly196**, **Asp199**, **Leu200**, **Val203**, **Gly205**, **Val207**, **Asn208**, **Leu209**, **Met226**, **Gly227**, **Asn263**, Gly295, Thr296, **Val297**, **Thr309**, **Val310**, **Ile311**
docked PC190723	**Gln192**, **Gly193**, **Gly196**, **Asp199**, **Leu200**, **Val203**, **Gly205**, **Val207**, **Asn208**, **Leu209**, **Met226**, **Gly227**, Leu261, **Asn263**, **Val297**, **Thr309**, **Val310**, **Ile311**

[a]The common residues of docked PC190723 and crystal PC190723 are shown in bold.

SB-RA-2001 was docked into the *Bs*FtsZ structure to determine the putative binding site and the residues of *Bs*FtsZ involved in the interaction with SB-RA-2001 (Figure 5). An analysis of the docking results indicated that SB-RA-2001 bound to FtsZ in a cleft region between helix H7 and the C-terminal domain. Further, the residues of *Bs*FtsZ within 4 Å of the SB-RA-2001 moiety were identified (Table 2), and the bold residues in Table 2 are the *Bs*FtsZ residues common to both PC190723 and SB-RA-2001 identified through docking analysis. SB-RA-2001 was forming hydrophobic and hydrogen bonding interactions with *Bs*FtsZ. The five residues of *Bs*FtsZ (E305, R191, Q192, N188, and N33) were observed to be hydrogen bonded to SB-RA-2001 (Figure 5). Because the mechanism of action of SB-RA-2001 was similar to that of PC190723,[13] we docked SB-RA-2001 on *Bs*FtsZ in combination with PC190723 (Figure 5). Interestingly, both SB-RA-2001 and PC190723 were found to bind to analogous binding pockets in *Bs*FtsZ and also to share some interacting residues (Table 2).

SB-RA-2001 Caused Growth Inhibition and Induced Filamentation in *B. subtilis* 168 and *M. smegmatis* Cells. SB-RA-2001 inhibited the proliferation of *B. subtilis* 168 and *M. smegmatis* cells in liquid culture with half-maximal inhibitory concentrations (IC_{50}) of 20 ± 1 and 18 ± 1 μM, respectively. However, SB-RA-2001 did not inhibit the proliferation of *E. coli* K12 cells in liquid culture. The effect of SB-RA-2001 on the growth of *B. subtilis* 168 and *M. smegmatis* cell proliferation was also measured by the standard colony counting method.[36] In control, the CFU was found to be (2.4 ± 1.2) × 10^6, and the CFU was reduced to (4.9 ± 0.7) × 10^5, (3.2 ± 0.4) × 10^4, and (1.2 ± 0.3) × 10^4 in the presence of 20, 25, and 35 μM SB-RA-2001, respectively (Figure S5 of the Supporting Information). However, no colony was observed in the presence of 38 μM SB-RA-2001, suggesting it to be the MIC value of SB-RA-2001 on *B. subtilis* 168 cells. Similarly, the CFU of *M. smegmatis* cells was found to be (5.7 ± 0.5) × 10^7, (11.7 ± 0.4) × 10^6, and (3.7 ± 0.4) × 10^5 in the absence of SB-RA-2001 and in the presence of 50 and 55 μM SB-RA-2001, respectively, and the MIC was estimated to be 60 μM. Previously, SB-RA-2001 was reported to inhibit the proliferation of clinical isolates of *Mtb* strains

dx.doi.org/10.1021/bi401356y | *Biochemistry* 2014, 53, 2979−2992

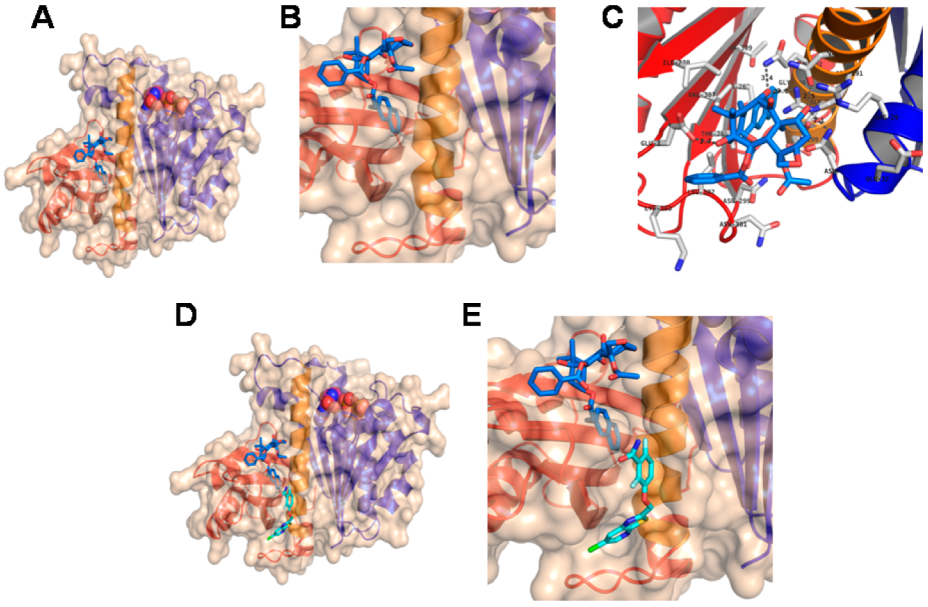

Figure 5. Analysis of the putative binding of SB-RA-2001 and PC190723 on *Bs*FtsZ. (A) The putative binding site of SB-RA-2001 on FtsZ is localized between helix H7 and the C-terminus of the *Bs*FtsZ monomer. (B) Magnified view of the SB-RA-2001 binding cavity. (C) Interaction of SB-RA-2001 with the surrounding amino acid residues of *Bs*FtsZ within 4 Å. (D) Binding sites of docked PC190723 (cyan) and SB-RA-2001 (sky blue) in *Bs*FtsZ. (E) Magnified view of the binding cavity.

Table 2. Residues of *Bs*FtsZ Lying within 4 Å of Docked Compounds[a]

PC190723 (docked)	**Asn33**, Gly34, Val35, Gln36, **Gln195**, **Asp199**, Thr203, Gly205, Leu206, Ser296, Val297, Ile298, **Asn299**, **Asn301**
SB-RA-2001	Arg29, Glu32, **Asn33**, Asn188, Arg191, Gln192, **Gln195**, Gly196, **Asp199**, Ile230, Asn263, Thr265, **Asn299**, **Asn301**, Leu302, Lys303, Glu305, Val307, Thr309

[a]The common residues of docked PC190723 and SB-RA-2001 are shown in bold.

H37Rv (drug-sensitive) and IMCJ946 K2 (multi-drug-resistant) with MICs of 5 and 1.25 μM, respectively.[22]

Further, SB-RA-2001 treatment induced strong filamentation in *B. subtilis* 168 (Figure 6) and *M. smegmatis* cells. The average cell lengths of *B. subtilis* 168 and *M. smegmatis* cells were determined to be 3.4 ± 1 and 2.8 ± 0.5 μm, respectively, in the absence of the compound. Upon treatment with 20 μM SB-RA-2001, the average cell lengths of *B. subtilis* 168 and *M. smegmatis* cells were found to be 42 ± 18 and 35 ± 25 μm, respectively. The lengths of vehicle-treated *B. subtilis* 168 cells were found to be in the range of 4−6 μm; however, SB-RA-2001-treated cells were highly elongated with a majority of the cells being in the range of 20−150 μm (Figure 6). These results suggested that SB-RA-2001 inhibited microbial proliferation by affecting the cytokinesis.

SB-RA-2001 Targeted Z-Ring Formation in *B. subtilis* 168 Cells. To determine whether inhibition of septum formation in *B. subtilis* 168 cells was due to the disruption in Z-ring formation, we examined the effects of SB-RA-2001 on Z-ring formation and nucleoid segregation (Figure 7). In the absence of SB-RA-2001, 68% of the *B. subtilis* 168 cells had Z-rings. However, SB-RA-2001 treatment strongly inhibited Z-ring formation in *B. subtilis* cells. For example, 20 and 17% of the cells had a Z-ring in the presence of 20 and 30 μM SB-RA-2001, respectively. Further, the number of Z-rings per micrometer of cell length was determined to be 0.15 ± 0.03, 0.03 ± 0.01, and 0.02 ± 0.01 in the absence of SB-RA-2001 and in the presence of 20 and 30 μM SB-RA-2001, respectively. The fluorescence of FtsZ (stained with the Cy3 secondary antibody) in the cells treated with SB-RA-2001 was found to be diffused and localized as spots and helices throughout the cell instead of a defined ring at the midcell (Figure 7).

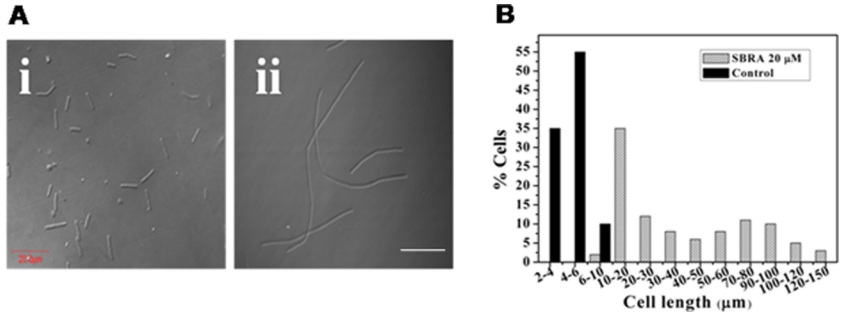

Figure 6. SB-RA-2001 induced filament formation in *B. subtilis* 168 cells. (A) *B. subtilis* 168 cells were grown in the presence of either vehicle (i) or 20 μM SB-RA-2001 (ii). The scale bar is 20 μm. (B) Histograms of the distribution of the length of control (vehicle-treated) and 20 μM SB-RA-2001-treated *B. subtilis* 168 cells.

dx.doi.org/10.1021/bi401356y | *Biochemistry* 2014, 53, 2979−2992

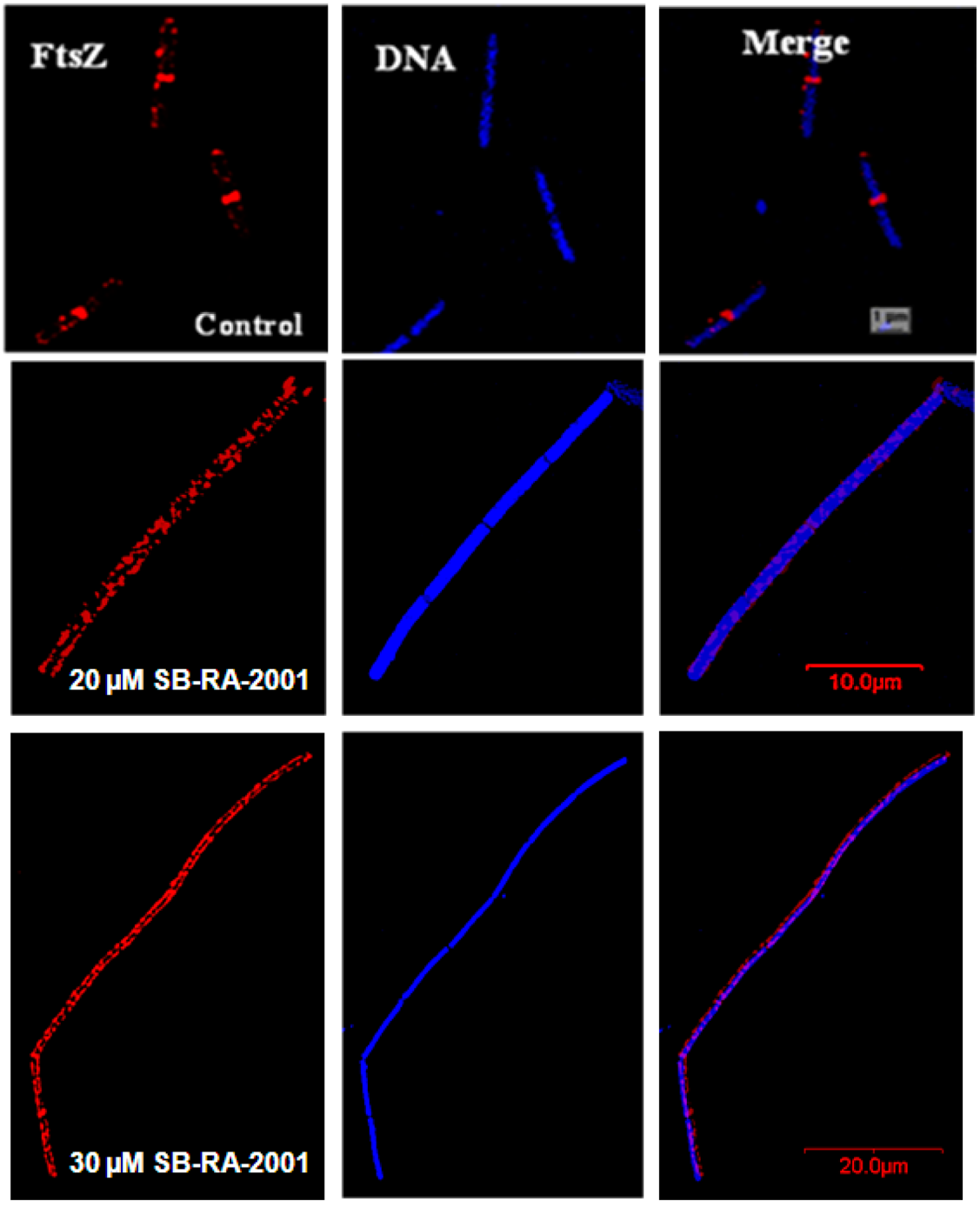

Figure 7. SB-RA-2001 perturbed Z-ring formation without affecting nucleoid segregation in *B. subtilis* 168 cells. *B. subtilis* 168 cells were incubated with vehicle (control) and 20 and 30 μM SB-RA-2001 for 4 h. Scales bars are 1, 10, and 20 μm, respectively.

Because the Z-ring acts as a scaffold for the recruitment of several cell division proteins, its perturbation is expected to affect their positioning at the midcell.[1] Therefore, the effect of SB-RA-2001 on the cellular localization of DivIVA, a protein that remains at both the poles and is recruited to the Z-ring at the onset of septal constriction, was examined.[44] In the untreated cells, GFP-tagged DivIVA showed the expected pattern of localization, i.e., at the midcell and poles, whereas DivIVA was mostly located at the two poles and was no longer recruited to the prospective cell division site in the SB-RA-2001-treated cells (Figure 8A). Moreover, the presence of punctate spots of DivIVA and FtsZ through the cell length indicated the presence of incomplete Z-ring formation in the presence of SB-RA-2001. The perturbed localization of DivIVA supported the finding that Z-ring formation was hampered in the presence of 20 μM SB-RA-2001. Further, the merged images of GFP-tagged DivIVA and Cy3-stained FtsZ also confirmed that FtsZ assembly at the midcell was affected.

Septum formation can be inhibited either by direct interference with the cell division machinery or by impaired nucleoid segregation.[45] The quantification of DNA in SB-RA-2001-treated cells was achieved using flow cytometric analysis. The median fluorescence intensity of propidium iodide-stained SB-RA-2001-treated cells was found to increase by several-fold

dx.doi.org/10.1021/bi401356y | *Biochemistry* 2014, 53, 2979−2992

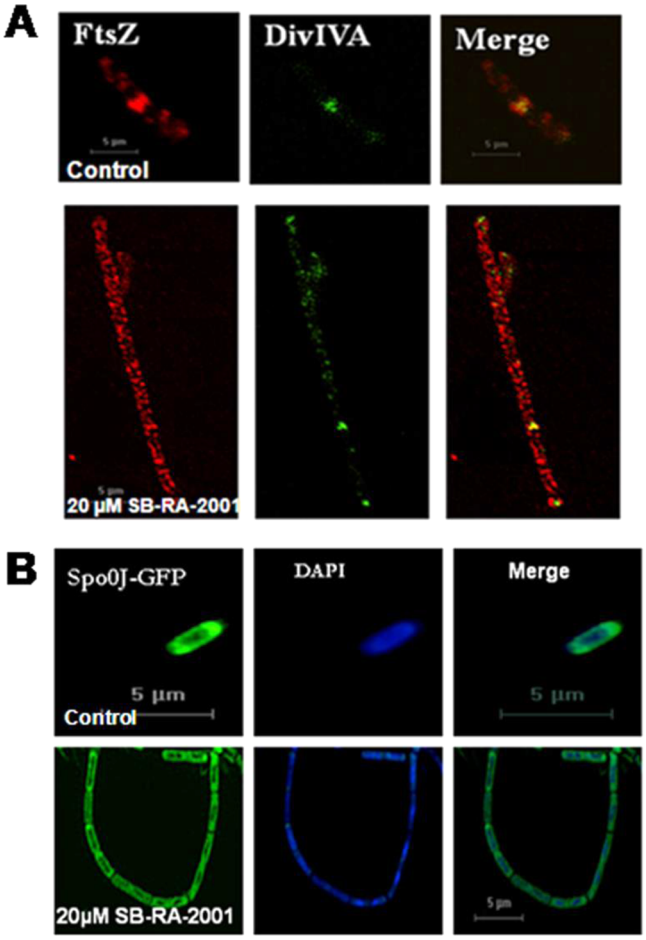

Figure 8. SB-RA-2001 delocalized GFP-DivIVA but did not influence the localization of GFP-tagged Spo0J in *B. subtilis* 168 cells. (A) Effects of SB-RA-2001 on the localization of GFP-DivIVA in *B. subtilis* 168 1803 cells. The scale bar is 5 μm. (B) Effects of SB-RA-2001 on the localization of GFP-tagged Spo0J in *B. subtilis* 168 strain HM160 cells. The scale bar is 5 μm.

compared to that of the vehicle-treated *B. subtilis* 168 cells, indicating that the average DNA content of SB-RA-2001-treated cells was much higher than that of the control cells (Figure S6 of the Supporting Information). SB-RA-2001 induced elongation of *B. subtilis* 168 cells (Figure 6), and these elongated cells harbored several copies of nucleoids (Figures 7 and 8B). The marked difference in the DNA content of the treated and control cells therefore indicated that the DNA duplication was not perturbed in the presence of SB-RA-2001 (Figure S6 of the Supporting Information). The effect of 20 μM SB-RA-2001 on nucleoid segregation was examined by staining the exponentially grown *B. subtilis* 168 cells with DAPI (Figure S7 of the Supporting Information). Most of the control cells had two nucleoids; 19, 75, and 6% of the control cells were found to have one, two, and four nucleoids, respectively. In the presence of 20 μM SB-RA-2001, single-nucleoid-containing cells were not found, 23% of the cells had two nucleoids, and 77% of the cells had four or more nucleoids. The frequency of the presence of nucleoids per micrometer of cell length was found to be nearly identical in the absence and presence of SB-RA-2001. For example, the number of nucleoids per micrometer of the cell length was determined to be 0.49 $\pm$ 0.1 and 0.4 $\pm$ 0.05 in the absence and presence of 20 μM SB-RA-2001, respectively, indicating that SB-RA-2001 had no appreciable effect on nucleoid segregation (Figure S7 of the Supporting Information). Further, the effect of SB-RA-2001 on the localization pattern of Spo0J was examined in *B. subtilis* cells.[45] Spo0J is a chromosomally associated protein, required for proper chromosomal partitioning, separation of sister origins, and synchronous DNA replication at the initiation of the DNA replication process.[46,47] Delocalization of Spo0J from either side of the nucleoid would indicate imperfect nucleoid segregation.[46,47] The localization pattern of Spo0J in SB-RA-2001-treated cells was found to be similar to that of the control cells (Figure 8B). The results together indicated that SB-RA-2001 might not have a discernible effect on nucleoid segregation.

SB-RA-2001 Did Not Perturb the Membrane Potential of *B. subtilis* 168 Cells. Vehicle-treated *B. subtilis* 168 cells displayed weak $DiOC_2$ fluorescence (Figure 9). As expected, a strong increase in $DiOC_2$ fluorescence was observed in the presence of CCCP (a positive control), indicating that CCCP treatment perturbed the membrane potential of *B. subtilis* 168 cells.[38,39] However, 20 and 30 μM SB-RA-2001-treated *B. subtilis* 168 cells showed emission spectra similar to that of the vehicle-treated cells, suggesting that SB-RA-2001 did not affect the membrane potential of *B. subtilis* 168 cells (Figure 9).

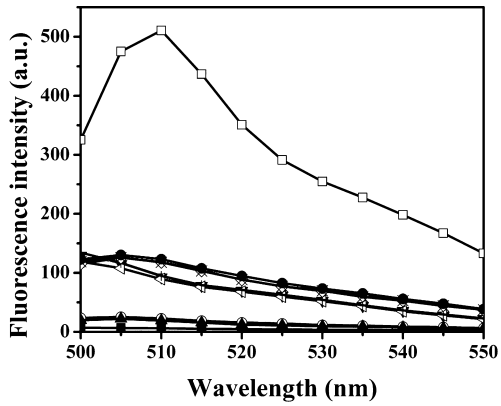

Figure 9. SB-RA-2001 did not affect the membrane potential of *B. subtilis* 168 cells. The fluorescence spectra of PBS (■), *B. subtilis* 168 cells (▲), and *B. subtilis* 168 cells in the presence of DMSO (○), only $DiOC_2$ (leftward-pointing triangles), 30 μM SB-RA-2001 in $DiOC_2$ (▼), and $DiOC_2$ in the presence of 0.2 μM CCCP (+) are shown. Also shown are spectra of the *B. subtilis* 168 cells without (●) and with 20 (×) and 30 μM (◇) SB-RA-2001 and 0.2 μM CCCP (□) in the presence of $DiOC_2$.

■ DISCUSSION

In this study, a taxane, SB-RA-2001, was found to effectively inhibit the proliferation of *B. subtilis* 168 and *M. smegmatis* cells and to induce filamentation in these cells. Further, SB-RA-2001 perturbed the formation of the Z-ring in *B. subtilis* 168 cells without disturbing nucleoid segregation. Moreover, it affected the localization of the late cell division protein, DivIVA, suggesting that it targeted FtsZ *in vivo*. *In vitro*, SB-RA-2001 bound to purified FtsZ, promoted its assembly, and reduced the GTPase activity of FtsZ, suggesting that SB-RA-2001 inhibited the proliferation of bacterial cells by perturbing the assembly dynamics of FtsZ. A computational analysis indicated that SB-RA-2001 binds to FtsZ in the interdomain cleft region between the C-terminal domain and helix H7. However, SB-RA-2001 did not have any effect on the assembly of tubulin *in vitro*. In

dx.doi.org/10.1021/bi401356y | *Biochemistry* 2014, 53, 2979−2992

addition, a fluorescence spectroscopy experiment indicated that SB-RA-2001 binds to tubulin very weakly. The saturation was not achieved even up to 400 μM SB-RA-2001. Because of the limited solubility and inner filter effect at high SB-RA-2001 concentrations, it was not possible to quantify the K_d of the interaction of tubulin and SB-RA-2001. The results together suggested that SB-RA-2001 binds to tubulin very weakly compared to its binding to FtsZ.

Paclitaxel and SB-RA-2001 showed markedly different effects on mammalian cell proliferation and on the assembly of tubulin *in vitro*. Under similar conditions, paclitaxel inhibited HeLa cell proliferation with an IC_{50} of 12 ± 2 nM while SB-RA-2001 inhibited HeLa cell proliferation with an IC_{50} of 45 ± 5 μM, indicating that the cytotoxicity of SB-RA-2001 against mammalian cells was 3750-fold weaker than that of paclitaxel. In addition, low concentrations of paclitaxel greatly enhanced the assembly of tubulin; in contrast, SB-RA-2001 did not enhance tubulin assembly (Figure 1). Furthermore, paclitaxel was reported to bind to microtubules strongly with an apparent binding constant of 0.87 μM,[42] while SB-RA-2001 does not appear to bind to tubulin effectively. The results together showed that compared to paclitaxel, SB-RA-2001 exerts only weak effects on tubulin assembly and mammalian cell proliferation.

It should be noted that SB-RA-2001 is different from paclitaxel because of the presence of the (*E*)-3-(naphtha-2-yl)acryloyl (2-NpCH═CHCO) group in place of the *N*-benzoylisoserine moiety at the C13 position of the paclitaxel molecule. The results indicated that the substitution at C13 contributed to the substantially different effects of SB-RA-2001 on FtsZ and tubulin. This structure−activity relationship analysis was further supported by an analysis in which the structures of tubulin and *Bs*FtsZ were superimposed on each other to obtain a clear view of a probable paclitaxel binding site on FtsZ. In this respect, the crystal structures of tubulin (PDB entry 1JFF) and *Bs*FtsZ (PDB entry 2RHL) were superimposed on each other and structurally aligned using PyMol to determine the residues of *Bs*FtsZ that were in the proximity of the paclitaxel binding site in tubulin. The *Bs*FtsZ residues close to the paclitaxel-like site projected to be bound by docked PC190723 and SB-RA-2001 have been highlighted (Table. 3). Interestingly, it was observed that there was no similarity between the identified residues of tubulin and FtsZ (Table 3), which were located within 4 Å of the paclitaxel binding site in tubulin.[13] The findings indicated the probable resistance of tubulin toward SB-RA-2001 compared to that of FtsZ.

SB-RA-2001 exhibited only weak fluorescence with the emission maximum at 440 nm. When FtsZ binds, the emission maximum was shifted to 400 nm (a blue shift of ∼40 nm), suggesting that the compound binds to FtsZ at a hydrophobic pocket. The increase in the fluorescence intensity of the SB-RA-2001−FtsZ complex as compared to that of free SB-RA-2001 is likely due to the immobilization of SB-RA-2001 in the hydrophobic pocket of FtsZ. Further, the GTP competition assay suggested that SB-RA-2001 binds at a location different from the GTP binding site on FtsZ. We propose that binding of SB-RA-2001 to FtsZ might favor the strengthened lateral interaction of FtsZ protofilaments, leading to an increase in the extent of bundling of FtsZ filaments. FtsZ forms dynamic polymers, and the dynamicity is regulated by the GTPase activity of FtsZ.[1] SB-RA-2001 enhanced the stability of FtsZ polymers, and the stable polymers led to the suppression of the GTP hydrolysis rate of FtsZ. Moreover, SB-RA-2001 inhibited

Table 3. Amino Acid Residues of β-Tubulin Lying within 4 Å of Paclitaxel and Residues of *Bs*FtsZ Lying within 4 Å of the Paclitaxel-like Site[a]

β-tubulin (PDB entry 1JFF)	*Bs*FtsZ (PDB entry 2RHL)
Glu22	Arg29
Val23	Glu32
Asp25	**Asn33**
Glu26	Glu185
Leu217	Asn188
Asp226	Arg191
His229	**Gln195**
Leu230	Ile230
Ala233	**Asn301**
Ser236	Glu305
Phe272	
Pro274	
Leu275	
Thr276	
Ser277	
Arg278	
Pro368	
Arg369	
Gly370	

[a]The residues of *Bs*FtsZ close to paclitaxel-like site projected to be bound by docked PC190723 and SB-RA-2001 are shown in bold.

the GTPase activity of FtsZ similarly in the absence and presence of detergent Triton X-100, suggesting that the inhibitory effect observed was not a consequence of the formation of colloids by SB-RA-2001. A recent study has suggested that some of the FtsZ-targeted compounds such as totarol, Zantrin Z1, and 4′-hydroxydichamanetin might inhibit the GTPase activity of FtsZ through the mechanism of self-aggregation of the compound.[19]

The mechanism of action of SB-RA-2001 on FtsZ resembled that of microtubule-stabilizing agent paclitaxel. *In vitro*, paclitaxel promotes tubulin assembly; however, in cells, it triggers cell death by stabilizing microtubules, which prevents the formation and functioning of the mitotic spindle.[48] In a similar manner, SB-RA-2001 also promoted the assembly and bundling of FtsZ protofilaments *in vitro* but perturbed the formation of Z-rings in cells. Similar effects were also shown by other FtsZ-stabilizing agents such as OTBA and PC190723; these agents promoted the bundling of FtsZ *in vitro* but prevented Z-ring formation in cells.[13,17] *In silico* analysis of binding of SB-RA-2001 to FtsZ indicated that the taxane derivative binds to *Bs*FtsZ in the interdomain cleft region, adjacent to helix H7. Helix H7 is an integral part of the *Bs*FtsZ structure and bridges the N- and C-terminal domains of FtsZ. Helix H7 in turn is anchored to the N- and C-terminal regions through H-bonded interactions between residues Arg29 and Asn188 and residues Gly196 and Asn263, respectively.[49] Interestingly, all four of these residues were involved in the binding interactions of SB-RA-2001 with *Bs*FtsZ. It is therefore predicted that the absence of the H-bonded interactions might have ruptured the interactions between N- and C-terminal domains. A similar mechanism of action was reported for the FtsZ-polymerizing agent, PC190723, in which the compound promoted FtsZ assembly and bound to a region similar to that of SB-RA-2001. Docking analysis suggested SB-RA-2001 and PC190723 may bind to analogous binding pockets on FtsZ (Figure 5 and Table 2), indicating a common mechanism of

dx.doi.org/10.1021/bi401356y | *Biochemistry* 2014, 53, 2979−2992

action for the two inhibitors. Moreover, PC190723 was reported to bind to FtsZ at a site that was comparable to the paclitaxel binding site in tubulin, and like the tubulin polymerization enhancing activity of paclitaxel, PC190723 also enhances the assembly of FtsZ. An analysis of the superimposition studies indicated that like PC190723, SB-RA-2001 also binds to FtsZ at a site that is similar to the paclitaxel binding domain in tubulin (Figure S8 of the Supporting Information). Therefore, SB-RA-2001 may stabilize FtsZ polymers through a mechanism that is similar to the mechanism of action of paclitaxel on microtubules.

The increased cell length of *B. subtilis* and *M. smegmatis* in the presence of SB-RA-2001 indicated that the compound inhibits cytokinesis in bacterial cells. Immunofluorescence experiments showed that SB-RA-2001 treatment perturbed Z-ring formation in *B. subtilis* 168 cells, and the number of Z-rings per unit cell length was considerably reduced in SB-RA-2001-treated cells. However, there was no change in nucleoid segregation, indicating that SB-RA-2001 did not target DNA in bacterial cells. Because the Z-ring is capable of generating force for bacterial cell division, its perturbation can block bacterial cell division, leading to elongated *B. subtilis* 168 cells.[50] We also found that upon SB-RA-2001 treatment, DivIVA was no longer recruited to the future cell division sites and was concentrated at the cell poles of *B. subtilis* cells. This finding suggested that DivIVA did not associate with the perturbed FtsZ ring wherein significant membrane constriction is absent. The structural role of DivIVA in the cell division of Gram-positive bacteria by recruiting other proteins to cell division sites has also been reported.[51,52] DivIVA was also reported to have essential roles in chromosome segregation and cell wall synthesis.[53] Moreover, the division site selection mechanism of the MinCD system was found to be regulated by DivIVA through an interacting protein MinJ.[54] An analysis of the structural domains of DivIVA revealed that it consists of a lipid binding N-terminal domain and a C-terminal domain.[55] While transmembrane protein MinJ was found to interact with the N-terminal domain of DivIVA, the C-terminal domain was involved in the binding interactions of RacA, a protein essential for chromosome segregation under sporulation conditions.[56] The perturbed localization of DivIVA in SB-RA-2001-treated *B. subtilis* cells indicated the formation of defective FtsZ rings. Spo0J is an initiation marker for DNA segregation in *B. subtilis* cells at the onset of DNA duplication.[57] The localization pattern of Spo0J was unaffected by the SB-RA-2001 treatment, indicating that the initiation of DNA replication was not hampered in the presence of SB-RA-2001. In addition, flow cytometric analysis indicated that DNA duplication was not stalled in the presence of SB-RA-2001 and the elongated cells harbored more copies of the nucleoids. In addition, the frequency of occurrence of nucleoids per micrometer of cell length was similar in both untreated and SB-RA-2001-treated cells, and DAPI staining of the SB-RA-2001-treated *B. subtilis* 168 cells indicated that the nucleoid segregation was not detectably perturbed in most of the cells. However, the possibility of some of the SB-RA-2001-treated elongated cells containing uneven DNA mass cannot be ruled out. The results suggested that SB-RA-2001 inhibited Z-ring formation by promoting FtsZ assembly and hyper-stabilizing FtsZ polymers. In addition, half-maximal inhibitory concentrations (IC_{50}) of SB-RA-2001 on bacterial cell and mammalian cell proliferation were determined to be 20 ± 1 and 45 ± 5 μM, respectively, indicating that SB-RA-2001 has more activity toward bacterial cells. The results together suggest that SB-RA-2001 would serve as a lead molecule and that further modification of its structure could help in the development of a potent taxane-based FtsZ-targeted antibacterial drug. In fact, C-seco analogues of SB-RA-2001 have been reported to be equally active against drug-sensitive and drug-resistant *Mtb* strains with negligible cytotoxicity.[5,6] Accordingly, it would be interesting and beneficial to investigate their activities and mechanism of action against various pathogens that are serious concerns to human health.

■ ASSOCIATED CONTENT

Supporting Information

The effect of SB-RA-2001 on the assembly kinetics of FtsZ (Figure S1), the effect of SB-RA-2001 on FtsZ assembly analyzed by electron and fluorescence microscopy (Figure S2), the effect of GTP on the binding of SB-RA-2001 to FtsZ (Figure S3), the superimposition of docked PC190723 on the crystallographically determined PC190723 structure of *Sa*FtsZ (Figure S4), the plot of CFU of *B. subtilis* 168 cells versus varying concentrations of SB-RA-2001 (Figure S5), the quantification of DNA in control and SB-RA-2001-treated cells by flow cytometric analysis (Figure S6), the effect of SB-RA-2001 on the nucleoid segregation of *B. subtilis* 168 cells (Figure S7), and the superimposition of the *Bs*FtsZ monomer on β-tubulin (Figure S8). This material is available free of charge via the Internet at http://pubs.acs.org.

■ AUTHOR INFORMATION

Corresponding Author

*Department of Biosciences and Bioengineering, Indian Institute of Technology Bombay, Powai, Mumbai 400076, India. Telephone: 91-22-2576-7838. Fax: 91-22-2572-3480. E-mail: panda@iitb.ac.in.

Author Contributions

D.S. and A.B. contributed equally to this work.

Funding

This study is partly supported by a grant from the Council of Scientific and Industrial Research, Government of India, to D.P. and partly by National Institutes of Health Grant AI 078251 to I.O. D.S. thanks DBT for a research associate fellowship.

Notes

The authors declare no competing financial interest.

■ ACKNOWLEDGMENTS

We thank the Indian Institute of Technology Bombay for providing the transmission electron microscopy facility and FACS facility.

■ ABBREVIATIONS

PIPES, piperazine-*N*,*N*′-bis(2-ethanesulfonic acid); PMSF, phenylmethanesulfonyl fluoride; DAPI, 6-diamidino-2-phenylindole; FITC, fluorescein isothiocyanate; IPTG, isopropyl β-D-1-thiogalactopyranoside; CFU, colony-forming units.

■ REFERENCES

(1) Adams, D. W., and Errington, J. (2009) Bacterial cell division: Assembly, maintenance and disassembly of the Z ring. *Nat. Rev. Microbiol.* 7, 642−653.

(2) Erickson, H. P., Anderson, D. E., and Osawa, M. (2010) FtsZ in bacterial cytokinesis: Cytoskeleton and force generator all in one. *Microbiol. Mol. Biol. Rev.* 74, 504−528.

(3) Barbero, C. S., Fontecha, M. M., Chacon, P., and Andreu, J. M. (2012) Targeting the Assembly of Bacterial Cell Division Protein FtsZ with Small Molecules. *ACS Chem. Biol. 7*, 269−277.
(4) Singh, P., and Panda, D. (2010) FtsZ inhibition: A promising approach for antistaphylococcal therapy. *Drug News Perspect. 23*, 295−304.
(5) Huang, Q., Tonge, P. J., Slayden, R. A., Kirikae, T., and Ojima, I. (2007) FtsZ: A novel target for tuberculosis drug discovery. *Curr. Top. Med. Chem. 7*, 527−543.
(6) Kumar, K., Awasthi, D., Berger, W. T., Tonge, P. J., and Ojima, I. (2010) Discovery of anti-TB agents that target the cell-division protein FtsZ. *Future Med. Chem. 2*, 1305−1323.
(7) Kapoor, S., and Panda, D. (2009) Targeting FtsZ for antibacterial therapy: A promising avenue. *Expert Opin. Ther. Targets 13*, 1037−1051.
(8) Jindal, B., Bhattacharya, A., and Panda, D. (2013) Inhibitors of bacterial cell partitioning. In *Antibiotics: Targets, Mechanisms and Resistance* (Gualerzi, C., Brandi, L., Fabbretti, A., and Pon, L., Eds.) pp 151−182, Wiley-VCH, Weinheim, Germany.
(9) Beuria, T. K., Santra, M. K., and Panda, D. (2005) Sanguinarine blocks cytokinesis in bacteria by inhibiting FtsZ assembly and bundling. *Biochemistry 44*, 16584−16593.
(10) Jaiswal, R., Beuria, T. K., Mohan, R., Mahajan, S. K., and Panda, D. (2007) Totarol inhibits bacterial cytokinesis by perturbing the assembly dynamics of FtsZ. *Biochemistry 46*, 4211−4220.
(11) Rai, D., Singh, J. K., Roy, N., and Panda, D. (2008) Curcumin inhibits FtsZ assembly: An attractive mechanism for its antibacterial activity. *Biochem. J. 410*, 147−155.
(12) Hemaiswarya, S., Soudaminikkutty, R., Narasumani, M. L., and Doble, M. (2011) Phenylpropanoids inhibit protofilament formation of *Escherichia coli* cell division protein FtsZ. *J. Med. Microbiol. 60*, 1317−1325.
(13) Andreu, J. M., Schaffner-Barbero, C., Huecas, S., Alonso, D., Lopez-Rodriguez, M. L., Ruiz-Avila, L. B., Nuñez-Ramirez, R., Llorca, O., and Martin-Galiano, A. J. (2010) The antibacterial cell division inhibitor PC190723 is a FtsZ polymer stabilizing agent which induces filament assembly and condensation. *J. Biol. Chem. 285*, 14239−14246.
(14) Kumar, K., Awasthi, D., Lee, S. Y., Zanardi, I., Ruzsicska, B., Knudson, S., Tonge, P. J., Slayden, R. A., and Ojima, I. (2011) Novel trisubstituted benzimidazoles, targeting Mtb FtsZ, as a new class of antitubercular agents. *J. Med. Chem. 54*, 374−381.
(15) Plaza, A., Keffer, J. L., Bifulco, G., Lloyd, J. R., and Bewley, C. A. (2010) Chrysophaentins A-H, antibacterial bisdiarylbutene macrocycles that inhibit the bacterial cell division protein FtsZ. *J. Am. Chem. Soc. 132*, 9069−9077.
(16) Margalit, D. N., Romberg, L., Mets, R. B., Hebert, A. M., Mitchison, T. J., Kirschner, M. W., and RayChaudhuri, D. (2004) Targeting cell division: Small-molecule inhibitors of FtsZ GTPase perturb cytokinetic ring assembly and induce bacterial lethality. *Proc. Natl. Acad. Sci. U.S.A. 101*, 11821−11826.
(17) Beuria, T. K., Singh, P., Surolia, A., and Panda, D. (2009) Promoting assembly and bundling of FtsZ as a strategy to inhibit bacterial cell division: A new approach for developing novel antibacterial drugs. *Biochem. J. 423*, 61−69.
(18) Singh, P., Jindal, B., Surolia, A., and Panda, D. (2012) A rhodanine derivative CCR-11 inhibits bacterial proliferation by inhibiting the assembly and GTPase activity of FtsZ. *Biochemistry 51*, 5434−5442.
(19) Anderson, D. E., Kim, M. B., Moore, J. T., O'Brien, T. E., Sorto, N. A., Grove, C. I., Lackner, L. L., Ames, J. B., and Shaw, J. T. (2012) Comparison of small molecule inhibitors of the bacterial cell division protein FtsZ and identification of a reliable cross-species inhibitor. *ACS Chem. Biol. 7*, 1918−1928.
(20) Sarcina, M., and Mullineaux, C. W. (2000) Effects of tubulin assembly inhibitors on cell division in prokaryotes in vivo. *FEMS Microbiol. Lett. 191*, 25−29.
(21) Ojima, I., Borella, C. P., Wu, X., Bounaud, P. Y., Oderda, C. F., Sturm, M., Miller, M. L., Chakravarty, S., Chen, J., Huang, Q., Pera, P., Brooks, T. A., Baer, M. R., and Bernacki, R. J. (2005) Design synthesis and SAR of novel taxane-based multi-drug resistance reversal agents. *J. Med. Chem. 48*, 2218−2228.
(22) Huang, Q., Kirikae, F., Kirikae, T., Pepe, A., Amin, A., Respicio, L., Slayden, R. A., Tonge, P. J., and Ojima, I. (2006) Targeting FtsZ for antituberculosis drug discovery: Noncytotoxic taxanes as novel antituberculosis agents. *J. Med. Chem. 49*, 463−466.
(23) Bradford, M. M. (1976) A rapid and sensitive method for the quantitation of microgram quantities of protein utilizing the principle of protein-dye binding. *Anal. Biochem. 72*, 248−254.
(24) Lu, C., Stricker, J., and Erickson, H. P. (1998) FtsZ from *Escherichia coli*, *Azotobacter vinelandii*, and *Thermotoga maritima*: Quantitation, GTP hydrolysis, and assembly. *Cell Motil. Cytoskeleton 40*, 71−86.
(25) Mukherjee, A., and Lutkenhaus, J. (1999) Analysis of FtsZ assembly by light scattering and determination of the role of divalent metal cations. *J. Bacteriol. 181*, 823−832.
(26) Jaiswal, R., Patel, R. Y., Asthana, J., Jindal, B., Balaji, P. V., and Panda, D. (2010) E93R substitution of *Escherichia coli* FtsZ induces bundling of protofilaments, reduces GTPase activity, and impairs bacterial cytokinesis. *J. Biol. Chem. 285*, 31796−31805.
(27) Yi, Q. M., and Lutkenhaus, J. (1985) The nucleotide sequence of the essential cell-division gene ftsZ of *Escherichia coli*. *Gene 36*, 241−247.
(28) Santra, M. K., and Panda, D. (2003) Detection of an intermediate during unfolding of bacterial cell division protein FtsZ: Loss of functional properties precedes the global unfolding of FtsZ. *J. Biol. Chem. 278*, 21336−21343.
(29) Geladopoulos, T. P., Sotiroudis, T. G., and Evangelopoulos, A. E. (1991) A malachite green colorimetric assay for protein phosphatase activity. *Anal. Biochem. 192*, 112−116.
(30) Morris, G. M., Huey, R., Lindstrom, W., Sanner, M. F., Belew, R. K., Goodsell, D. S., and Olson, A. J. (2009) Autodock4 and AutoDockTools4: Automated docking with selective receptor flexiblity. *J. Comput. Chem. 16*, 2785−2791.
(31) Schüttelkopf, A. W., and van Aalten, D. M. (2004) PRODRG: A tool for high-throughput crystallography of protein-ligand complexes. *Acta Crystallogr. D60*, 1355−1363.
(32) Raymond, A., Lovell, S., Lorimer, D., Walchli, J., Mixon, M., Wallace, E., Thompkins, K., Archer, K., Burgin, A., and Stewart, L. (2009) Combined protein construct and synthetic gene engineering for heterologous protein expression and crystallization using Gene Composer. *BMC Biotechnol. 9*, 37.
(33) Tan, C. M., Therien, A. G., Lu, J., Lee, S. H., Caron, A., Gill, C. J., Lebeau-Jacob, C., Benton-Perdomo, L., Monteiro, J. M., Pereira, P. M., Elsen, N. L., Wu, J., Deschamps, K., Petcu, M., Wong, S., Daigneault, E., Kramer, S., Liang, L., Maxwell, E., Claveau, D., Vaillancourt, J., Skorey, K., Tam, J., Wang, H., Meredith, T. C., Sillaots, S., Wang-Jarantow, L., Ramtohul, Y., Langlois, E., Landry, F., Reid, J. C., Parthasarathy, G., Sharma, S., Baryshnikova, A., Lumb, K. J., Pinho, M. G., Soisson, S. M., and Roemer, T. (2012) Restoring methicillin-resistant *Staphylococcus aureus* susceptibility to β-lactam antibiotics. *Sci. Transl. Med. 4* (126), 126ra35.
(34) DeLano, W. L. (2002) *The PyMOL Molecular Genetics Graphics System*, DeLano Scientific LLC, San Carlos, CA.
(35) Löwe, J., Li, H., Downing, K. H., and Nogales, E. (2001) Refined structure of $\alpha\beta$-tubulin at 3.5 Å resolution. *J. Mol. Biol. 313* (5), 1045−1057.
(36) Wiegand, I., Hilpert, K., and Hancock, R. E. (2008) Agar and broth dilution methods to determine the minimal inhibitory concentration (MIC) of antimicrobial substances. *Nat. Protoc. 3*, 163−175.
(37) Foss, M. H., Eun, Y. J., Grove, C. I., Pauw, D. A., Sorto, N. A., Rensvold, J. W., Pagliarini, D. J., Shaw, J. T., and Weibel, D. B. (2013) Inhibitors of bacterial tubulin target bacterial membranes in vivo. *MedChemComm 4*, 112−119.
(38) Hargittai, P. T., Youmans, S. J., and Lieberman, E. M. (1991) Determination of the membrane potential of cultured mammalian Schwann cells and its sensitivity to potassium using a thiocarbocyanine fluorescent dye. *Glia 4*, 611−616.

(39) Shapiro, H. M. (2000) Membrane potential estimation by flow cytometry. *Methods 21*, 271−279.
(40) Rai, A., Gupta, T. K., Kini, S., Kunwar, A., Surolia, A., and Panda, D. (2013) CXI-benzo-84 reversibly binds to tubulin at colchicine site and induces apoptosis in cancer cells. *Biochem. Pharmacol. 86*, 378−391.
(41) Skehan, P., Storeng, R., Scudiero, D., Monks, A., McMahon, J., Vistica, D., Warren, J. T., Bokesch, H., Kenney, S., and Boyd, M. R. (1990) New colorimetric cytotoxicity assay for anticancer-drug screening. *J. Natl. Cancer Inst. 82*, 1107−1112.
(42) Parness, J., and Horwitz, S. B. (1981) Taxol binds to polymerized tubulin *in vitro*. *J. Cell Biol. 91*, 479−487.
(43) Kukol, A. (2008) Molecular modeling of proteins. In *Methods in Molecular Biology* (Kukol, A., Ed.) Vol. *443*, Humana Press, Totowa, NJ.
(44) Jacobs, C., and Shapiro, L. (1999) Bacterial cell division: A moveable feast. *Proc. Natl. Acad. Sci. U.S.A. 96*, 5891−5893.
(45) Sass, P., Jostena, M., Famulla, K., Schiffer, G., Sahl, H. G., Hamoen, L., and Brotz-Oesterhelt, H. (2011) Antibiotic acyldepsipeptides activate ClpP peptidase to degrade the cell division protein FtsZ. *Proc. Natl. Acad. Sci. U.S.A. 108*, 17474−17479.
(46) Lee, P. S., and Grossman, A. D. (2006) The chromosome partitioning proteins Soj (ParA) and Spo0J (ParB) contribute to accurate chromosome partitioning, separation of replicated sister origins, and regulation of replication initiation in *Bacillus subtilis*. *Mol. Microbiol. 60*, 853−869.
(47) Murray, H., and Errington, J. (2008) Dynamic control of the DNA replication initiation protein DnaA by Soj/ParA. *Cell 135*, 74−84.
(48) Dumontet, C., and Jordan, M. A. (2010) Microtubule-binding agents: A dynamic field of cancer therapeutics. *Nat. Rev. Drug Discovery 9*, 790−803.
(49) Elsen, N. L., Lu, J., Parthasarathy, G., Reid, J. C., Sharma, S., Soisson, S. M., and Lumb, K. J. (2012) Mechanism of action of the cell-division inhibitor PC190723: Modulation of FtsZ assembly cooperativity. *J. Am. Chem. Soc. 134*, 12342−12345.
(50) Dajkovic, A., and Lutkenhaus, J. (2006) Z ring as executor of bacterial cell division. *J. Mol. Microbiol. Biotechnol. 11*, 140−151.
(51) Eswaramoorthy, P., Erb, M. L., Gregory, J. A., Silverman, J., Pogliano, K., Pogliano, J., and Ramamurthi, K. S. (2011) Cellular architecture mediates DivIVA ultrastructure and regulates Min activity in *Bacillus subtilis*. *mBio 2*, 257−268.
(52) Lenarcic, R., Halbedel, S., Visser, L., Shaw, M., Wu, L. J., Errington, J., Marenduzzo, D., and Hamoen, L. W. (2009) Localisation of DivIVA by targeting to negatively curved membranes. *EMBO J. 28*, 2272−2282.
(53) van Baarle, S., Celik, I. N., Kaval, K. G., Bramkamp, M., Hamoen, L. W., and Halbedel, S. (2013) Protein-protein interaction domains of *Bacillus subtilis* DivIVA. *J. Bacteriol. 195*, 1012−1021.
(54) Patrick, J. E., and Kearns, D. B. (2008) MinJ (YvjD) is a topological determinant of cell division in *Bacillus subtilis*. *Mol. Microbiol. 70*, 1166−1179.
(55) Oliva, M. A., Halbedel, S., Freund, S. M., Dutow, P., Leonard, T. A., Veprintsev, D. B., Hamoen, L. W., and Löwe, J. (2010) Features critical for membrane binding revealed by DivIVA crystal structure. *EMBO J. 29*, 1988−2001.
(56) Ben-Yehuda, S., Rudner, D. Z., and Losick, R. (2003) RacA, a bacterial protein that anchors chromosomes to the cell poles. *Science 299*, 532−536.
(57) Gruber, S., and Errington, J. (2009) Recruitment of condensin to replication origin regions by ParB/SpoOJ promotes chromosome segregation in *B. subtilis*. *Cell 137*, 685−696.